applied sciences

MDPI

Article

Continuous-Wave and Mode-Locked Operation of an In-Band Pumped Tm,Ho,Lu:$CaGdAlO_4$ Laser

Huangjun Zeng [1,2], Wenze Xue [1,2], Robert T. Murray [1,3], Weidong Chen [1,2], Zhongben Pan [4], Li Wang [1,5,6], Chen Cui [1,7], Pavel Loiko [8], Xavier Mateos [9], Uwe Griebner [1] and Valentin Petrov [1,*]

1 Max Born Institute for Nonlinear Optics and Ultrafast Spectroscopy, Max-Born-Str. 2a, 12489 Berlin, Germany
2 Fujian Institute of Research on the Structure of Matter, Chinese Academy of Sciences, Fuzhou 350002, China
3 Femtosecond Optics Group, Department of Physics, Imperial College London, Prince Consort Road, London SW7 2BW, UK
4 School of Information Science and Engineering, Shandong University, Qingdao 266237, China
5 Anhui Institute of Optics and Fine Mechanics, Chinese Academy of Sciences, Hefei 230031, China
6 Hefei Institute of Physical Science, Chinese Academy of Sciences, Hefei 230031, China
7 Research Center for Crystal Materials, Xinjiang Key Laboratory of Electronic Information Materials and Devices, Xinjiang Technical Institute of Physics & Chemistry, Chinese Academy of Sciences, Urumqi 830011, China
8 Centre de Recherche Sur Les Ions, Les Matériaux et la Photonique (CIMAP), UMR625 CEA-CNRS-ENSICAEN, Université de Caen, 6 Boulevard Maréchal Juin, CEDEX 4, 14050 Caen, France
9 Física i Cristal·lografia de Materials (FiCMA), Universitat Rovira i Virgili (URV), 43007 Tarragona, Spain
* Correspondence: petrov@mbi-berlin.de

Abstract: We investigate in-band pumping of a Tm,Ho,Lu:$CaGdAlO_4$ laser using a Raman-shifted Er-fiber laser (1678 nm), in the continuous-wave (CW) and mode-locked (ML) regimes. A maximum output power of 524 mW is obtained in the CW regime with a 5% output coupler at an absorbed pump power of 2.04 W, corresponding to a slope efficiency of 27.9%. A maximum CW wavelength tuning range of 160 nm at the zero level, from 1984 to 2144 nm, is obtained with a 0.2% output coupler. In the ML regime, pumping with 5.5 W (unpolarized), the average output power (0.2% output coupler) reaches 148 mW at a repetition rate of ~96 MHz. The output spectrum is centered at 2071.5 nm with a FWHM of 21.5 nm (σ-polarization). The pulse duration amounts to 218 fs (time-bandwidth product equal to 0.327).

Keywords: mode-locking; Ho laser; $CaGdAlO_4$; inhomogeneous broadening; disordered crystal; mixed crystal; in-band pumping; femtosecond pulses; co-doped crystal

Citation: Zeng, H.; Xue, W.; Murray, R.T.; Chen, W.; Pan, Z.; Wang, L.; Cui, C.; Loiko, P.; Mateos, X.; Griebner, U.; et al. Continuous-Wave and Mode-Locked Operation of an In-Band Pumped Tm,Ho,Lu:$CaGdAlO_4$ Laser. *Appl. Sci.* **2023**, *13*, 12927. https://doi.org/10.3390/app132312927

Academic Editor: Andrea Li Bassi

Received: 14 November 2023
Revised: 28 November 2023
Accepted: 1 December 2023
Published: 3 December 2023

1. Introduction

The tetragonal calcium aluminate $CaLnAlO_4$ crystals where Ln^{3+} denotes Gd^{3+} or Y^{3+} [1–3] represent one of the most interesting recently studied laser host materials families. The Gd compound is abbreviated in the literature as CALGO (or CGA) and the Y compound as CALYO (or CYA). Both crystallize in a K_2NiF_4-type structure with the Ca^{2+} and Ln^{3+} cations statistically distributed over the same Wyckoff site (4*e*, C_{4v}-symmetry) leading to structural disorder [4,5]. Doped with laser-active trivalent rare-earth (RE^{3+}) ions, such as Yb^{3+}, Tm^{3+}, Ho^{3+}, etc., these crystals exhibit inhomogeneous broadening of the absorption and emission spectral bands [6]. In contrast to the well-known disordered cubic garnets, however, disordered $CaLnAlO_4$ crystals possess relatively high thermal conductivity (~6.7 $Wm^{-1}K^{-1}$ for CALGO) with moderate dependence on the RE^{3+} doping level [7]. The emission of such lasers is polarized [8] due to the natural birefringence of the host crystals [9]. RE^{3+} doping is relatively easy due to the presence of passive Ln sites and both compounds melt congruently which facilitates large crystal growth by the conventional Czochralski (Cz) method [10].

The spectroscopic properties of RE^{3+}-doped $CaLnAlO_4$ render these materials excellent candidates for femtosecond pulse generation and amplification [11,12] with power scaling [13], including thin-disk geometries [14,15], facilitated by the good thermal conductivity. While most of the past ultrafast laser research focused on Yb^{3+}-doping with emission in the ~1 μm spectral range [11–15], more recently the interest is shifting towards Tm^{3+} and Ho^{3+} dopant ions with emission around 2 μm [16]. Co-doping of the $CaLnAlO_4$ crystals with Tm,Ho [17] is of special importance because the emission of Tm alone in this type of relatively weak ligand field crystals lies below 2 μm, in a wavelength range of structured water vapor absorption, which complicates the spectral support of broad bandwidths. In fact, Tm,Ho:CALGO and Tm,Ho:CALYO have been some of the most successful materials employed so far in femtosecond 2 μm lasers [16].

Lu^{3+} is another passive host-forming cation in many oxide materials and due to the close ionic radii of Lu^{3+} and Yb^{3+} or Tm^{3+} ions, such crystals are more easily doped and the thermal conductivity is less sensitive to the doping level compared to the Gd-containing counterparts, which are more suitable for doping with Nd^{3+}. However, $CaLuAlO_4$ could not be synthesized as a single crystal [18], and the obvious remaining option is to grow "mixed" or passive ion doped host crystals. The choice of Lu^{3+}:$CaGdAlO_4$ as a passive host crystal, with a partial substitution of Gd^{3+} by Lu^{3+}, is justified because due to the larger difference in the ionic radii (compared to Lu^{3+} and Y^{3+}), one can expect more inhomogeneous spectral line broadening as a result of the additional compositional disorder. Such mixed host crystals were employed for the first time in [19] with Yb-doping and in [20] with Tm-doping. Note that Lu doping levels of 5.2–5.5% as used in [19,20] have a similar disordering effect as the active ion doping itself. However, especially in the case of Tm^{3+}, with its complex multi-level energy scheme, excessively increasing the active ion doping concentration may lead to undesirable excited state interactions and fluorescence quenching.

Very recently, we carried out a comprehensive characterization of Cz grown Tm,Ho,Lu:CALGO crystals [21,22] and demonstrated continuous-wave (CW) [22] and mode-locked (ML) [23] laser operation under conventional ~800 nm pumping of the Tm^{3+} ion followed by energy transfer to the Ho^{3+} dopant.

Traditionally, Tm^{3+},Ho^{3+} co-doped materials are pumped around 0.8 μm (the $^3H_6 \rightarrow {}^3H_4$ Tm^{3+} transition in absorption); see Figure 1. This wavelength range can be readily addressed by high-brightness tunable Ti:Sapphire lasers and high-power spatially multimode AlGaAs semiconductor laser diodes. After excitation to the $^3H_4$ state, Tm^{3+} ions can experience two subsequent multiphonon non-radiative (NR) relaxation steps ending in the metastable (long-living) $^3F_4$ state. Another route to populate this manifold is the cross-relaxation (CR) process for adjacent Tm^{3+} ions, $^3H_4 + {}^3H_6 \rightarrow {}^3F_4$ and $^3F_4$, which enhances the pump quantum efficiency for Tm^{3+} ions by up to 2 (two-for-one process). Due to the nearly resonant energetic position of the $^3F_4$ Tm^{3+} and $^5I_7$ Ho^{3+} multiplets (the barycenter of the former multiplet exhibits a slightly higher energy), a bidirectional $Tm^{3+} \leftrightarrow Ho^{3+}$ energy transfer is observed. The lifetimes of the two involved excited states are represented by a single thermal equilibrium value and their populations are linked. Usually, the Ho:Tm co-doping ratio is selected between 1:10 to 1:5 to ensure efficient population of the upper laser level $^5I_7$ Ho^{3+} manifold.

Compared to single Ho^{3+} doping, the Tm^{3+},Ho^{3+} co-doping brings the advantage of easier pumping (namely, more accessible pump sources and higher pump absorption efficiencies). Its main limitation is the relatively high heat loading causing more severe thermal problems and thermal roll over in the output dependences and leading eventually to thermal fracture/laser ceasing, thus limiting the output power that can be extracted. The main sources of heat generation in Tm,Ho lasers pumped at 0.8 μm are (i) NR relaxation from the $^3H_4$ and $^3H_5$ Tm^{3+} levels (which is especially significant for oxide crystals with high phonon energies), (ii) energy-transfer upconversion (ETU) from the $^3F_4$ Tm^{3+} and $^5I_7$ Ho^{3+} excited states, and (iii) energy losses associated with the bidirectional $Tm^{3+} \leftrightarrow Ho^{3+}$ energy-transfer. The two relevant ETU processes are $^3F_4$(Tm) + $^3F_4$(Tm) $\rightarrow {}^3H_4$(Tm)

+ $^3H_6$(Tm) and $^3F_4$(Tm) + $^5I_7$(Ho) → $^3H_6$(Tm) + $^5I_5$(Ho). Both of these ETU processes are followed by multiple NR relaxation steps contributing to heat generation.

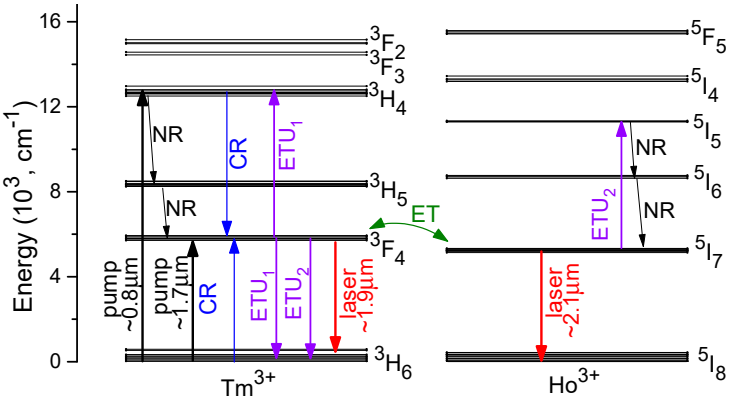

Figure 1. Energy level schemes of Tm^{3+} and Ho^{3+} in the $CaGdAlO_4$ crystal: black and red arrows–pump and laser transitions, respectively, CR–cross-relaxation, ETU–energy-transfer upconversion, ET–non-radiative energy transfer, NR–multi-phonon non-radiative relaxation.

Compared to the traditional Tm^{3+}-ion pumping near 0.8 μm, direct excitation of Tm^{3+} ions at ~1.7 μm to the $^3F_4$ state ($^3H_6$ → $^3F_4$, in-band or resonant pumping) can partially release the heat load. This mainly happens through suppression of the NR relaxation path from the $^3H_4$ and $^3H_5$ excited-states of Tm^{3+} [24]. The pump sources that address the spectral range of 1.7 μm are Raman-shifted Erbium fiber lasers and short wavelength Tm fiber lasers. They benefit from good beam quality (nearly diffraction limited pump beams) offering good prospects for reducing the laser threshold, boosting the laser efficiency and eventually power scaling of Tm,Ho lasers (as compared to traditional AlGaAs diode lasers). In the present work, we demonstrate the potential of the Tm in-band pumping scheme for tunable and ML Tm,Ho lasers benefiting from the combined gain bandwidths of the two active ions and the reduced heat load. A Tm^{3+},Ho^{3+} co-doped Lu^{3+}:$CaGdAlO_4$ aluminate crystal is selected as a reference gain material.

2. Materials and Methods

The tetragonal CALGO is an optically positive ($n_e > n_o$) uniaxial crystal. Thus, the spectroscopic properties of the dopant ions are described in terms of π ($E//c$) and σ ($E\perp c$) polarizations. The maximum absorption for the $^3H_6$ → $^3H_4$ Tm^{3+} transition in Tm,Ho,Lu:CALGO (Tm: 4.48%, Ho: 0.54%, Lu: 5.51%) from the ground level amounts to ~5.1 cm^{-1} close to 1700 nm for π-polarization and the corresponding bandwidth (FWHM) of this absorption band exceeds 100 nm [22]. The measured thermal equilibrium luminescence lifetime is 4.35 ms, for both ions emission near 2 μm [22].

As a pump source, we employed a home-made fiber Raman laser delivering 6 W of CW power at a central wavelength of 1678 nm, well matching the absorption peak of Tm^{3+} in CALGO, with a spectral FWHM of 0.8 nm. The laser consists of an input fiber Bragg grating (highly reflective at 1678 nm and highly transmissive at 1560 nm) spliced to 390 m of OFS Raman fiber (non-polarization maintaining) with a flat fiber cleave (0° angle at fiber end) providing ~4% feedback from the Fresnel reflection at the glass-air interface. The Raman cavity is pumped by a 12 W CW Er-fiber filtered amplified spontaneous emission source centered at 1560 nm, spliced directly to the Raman cavity. A high power fiber isolator (1550 nm) is used between the Er:fiber source output and the Raman cavity, to prevent back reflected 1550 nm radiation from the flat cleave at the output of the OFS Raman fiber damaging the Er-fiber pump source. The entire source is fiber integrated, and an f = 15.26 mm aspheric lens is used to collimate the fiber Raman laser at the flat cleave output. The source provides a stable and diffraction limited pump beam.

A 6 mm long, *a*-cut and antireflection (AR)-coated Tm,Ho,Lu:CALGO crystal with the above composition was used at normal incidence. The lateral dimensions were 4 (*a*) × 4 (*c*) mm^2. It was wrapped in indium foil and water cooled to 12 °C in a copper holder.

The maximum available pump power from the unpolarized fiber source after the imaging lenses and the pump mirror M_1, see Figure 2, was 5.5 W. External polarizers had to be used to record the input-output characteristics at constant spatial quality with the pump laser kept at maximum power. The Tm,Ho,Lu:CALGO sample was mounted with its *c*-axis vertical and it was pumped in π-polarization for higher absorption. A polarizer was first used to impose linear polarization to the pump, followed by a combination of a half-wave plate and a second polarizer acting as an attenuator.

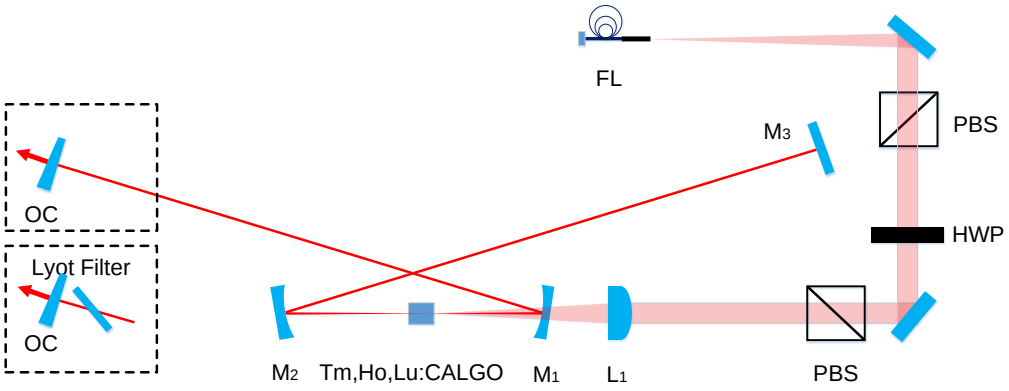

Figure 2. Experimental set up of the CW Tm,Ho,Lu:CALGO laser. Pump laser: Raman-shifted Er Fiber Laser (FL); L_1: AR coated plano-convex lens (f = 75 mm); M_1-M_2: concave dichroic mirrors (Radius of Curvature, RoC = −100 mm); M_3: flat rear total reflector; OC: wedged output coupler. PBS: polarization beam splitters. HWP: half-wave plate.

3. Continuous-Wave (CW) Laser Results

The CW laser performance of the Tm,Ho,Lu:CALGO crystal was studied with the four mirror laser cavity shown in Figure 2. The pump waist radius in the position of the crystal was measured to be w_P = 18 μm in both planes. The values for the laser beam radius calculated by the ABCD formalism were w_L = 33 and 36 μm in the sagittal and tangential planes, respectively. The single pass pump absorption was estimated under lasing conditions by measuring the residual power behind M_2. It depended only weakly on the OC transmission T_{OC} and varied from 66.2% to 85.9%, as a function of the incident power (due to the recycling effect), as shown in Figure 3a.

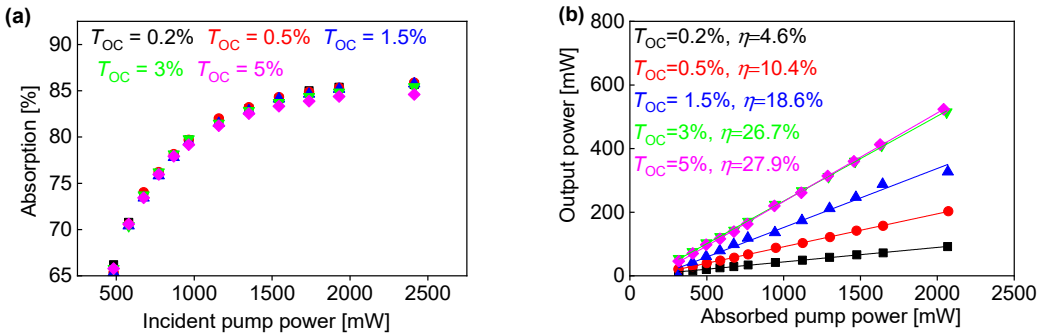

Figure 3. (**a**) Single pass pump absorption under lasing conditions vs. OC transmission, T_{OC}; (**b**) input–output characteristics of the CW Tm,Ho,Lu:CALGO laser for different OCs. The laser is naturally π-polarized (vertical).

Five different OCs were used to evaluate the laser performance in the CW regime, as shown in Table 1 and Figure 3b. The lowest threshold for CW operation was 124 mW with respect to the absorbed pump power using the lowest T_{OC} = 0.2%. A maximum output

power of 524 mW was obtained with the highest 5% OC at an absorbed pump power of ~2.04 W, corresponding to a slope efficiency of η = 27.9%.

Table 1. Pump threshold, P_{th}, maximum absorbed pump power, P_{abs}, and absorption, A, maximum output power, P_{out}, and slope efficiency, η, of the CW Tm,Ho,Lu:CALGO laser vs. OC transmission, T_{OC}.

T_{OC} (%)	P_{th} [mW]	P_{abs} (mW)	A (%)	P_{out} (mW)	η (%)
0.2	124	2067	85.7	92	4.60
0.5	130	2072	85.9	203	10.4
1.5	133	2069	85.8	327	18.6
3.0	164	2061	85.4	515	26.7
5.0	253	2041	84.6	524	27.9

The laser output spectra shown in Figure 4a were measured with a resolution better than 1 nm. The laser central wavelength in the CW regime varied with the transmission of the OC from 2079 to 2087 nm. This wavelength shift is expected for the three-level laser systems of Tm^{3+} and Ho^{3+}, where reabsorption increases at lower inversion rates when using lower OC transmission, and it is also in line with the gain spectra for π-polarization. All CW laser results for the different OCs are summarized in Table 1.

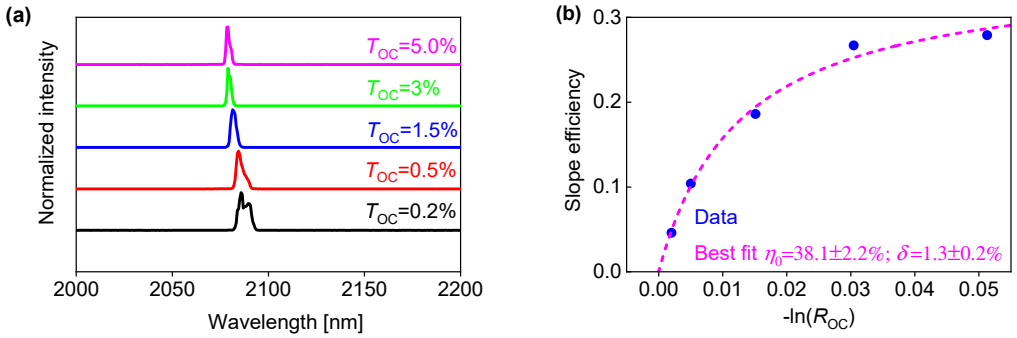

Figure 4. (**a**) CW laser output spectra vs. OC transmission; (**b**) slope efficiency as a function of the OC reflectivity $R_{OC} = 1 - T_{OC}$. The laser is naturally π-polarized (vertical).

The total round-trip resonator losses δ (reabsorption losses excluded), as well as the intrinsic slope efficiency η_0 (accounting for the mode matching and quantum efficiencies), were estimated with the Caird analysis [25] by fitting the measured slope efficiency as a function of the OC reflectivity R_{OC}. The fitting results and the best fit curve are shown in Figure 4b, giving the values of η_0 = 38.1% and δ = 1.3%.

The above CW laser wavelengths are above the limit of ~2075 nm established in previous experiments with 800 nm pumping [23], below which the naturally selected polarization switches from π to σ due to the rather close combined gain cross sections for the two principal polarizations [22]. Indeed, we established that in all cases the output polarization of the CW Tm,Ho,Lu:CALGO laser was parallel to the crystal *c* axis.

The wavelength tuning performance of the Tm,Ho,Lu:CALGO laser in the CW regime was studied by inserting a Lyot filter (3 mm thick quartz plate with a diameter of 20 mm and the optical axis at 60° to the surface) in the arm containing the OC, at an incident pump power of 2.5 W (pump π-polarization). The Brewster angle of the Lyot filter was in the horizontal plane so that it enforced laser oscillation in σ-polarization. The recorded tuning curves are shown in Figure 5a,b for two different OCs. They are rather smooth and without any gaps. A maximum wavelength tuning range of 160 nm at the zero level, from 1984 to 2144 nm, was obtained with the 0.2% OC. A slightly narrower wavelength tuning range of 158 nm, from 1985 nm to 2143 nm, was obtained with the 0.5% OC, which provided higher output power.

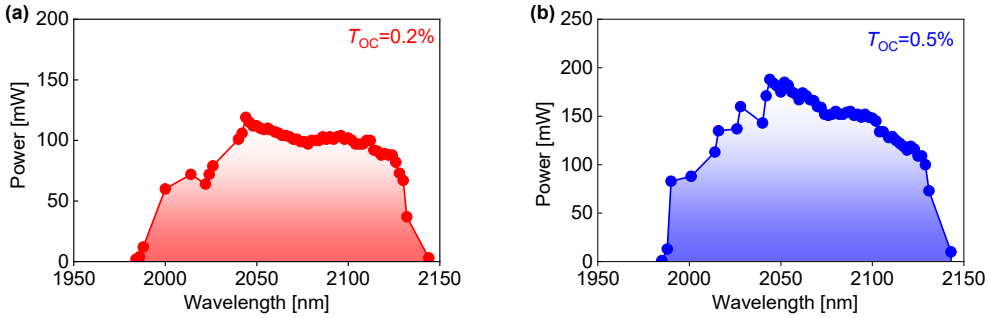

Figure 5. (**a**,**b**) spectral tuning curves in the CW regime obtained with a Lyot filter at 2.5 W incident pump power for T_{OC} = 0.2% and 0.5%. The laser is σ-polarized due to the insertion of the Lyot filter.

4. Mode-Locked (ML) Laser Results

To study mode-locking of the Tm,Ho,Lu:CALGO laser, the sample was mounted in the same way as for the CW laser studies, i.e., with its *c*-axis vertical, however, in order to utilize the full pump power available (5.5 W unpolarized) the polarizer and attenuator in Figure 2 were removed. The modified experimental set up shown in Figure 6 includes a SEmiconductor Saturable Absorber Mirror (SESAM), used as a rear reflector, and three dispersive mirrors (DM) for realization of a soliton like regime at negative overall cavity group delay dispersion (GDD). All DMs were specified with a GDD of −125 fs^2 per bounce. Four bounces on each of the plane DM_1 and DM_2 and two bounces on the curved (RoC = −100 mm) DM_3 per cavity round trip provide a total negative GDD of −1250 fs^2. DM_3 simultaneously serves to create a second cavity waist with a sufficiently small size for saturation of the SESAM absorption. The estimated radii of this second beam waist on the SESAM were w_L = 114 and 149 µm in the sagittal and tangential planes, respectively. In this cavity configuration, and using the full pump power, we measured the output power as a reference with the T_{OC} = 0.2% OC and the SESAM substituted by a plane totally reflecting mirror. The output power was 360 mW for an estimated absorbed power of 3.84 W distributed between the two polarizations.

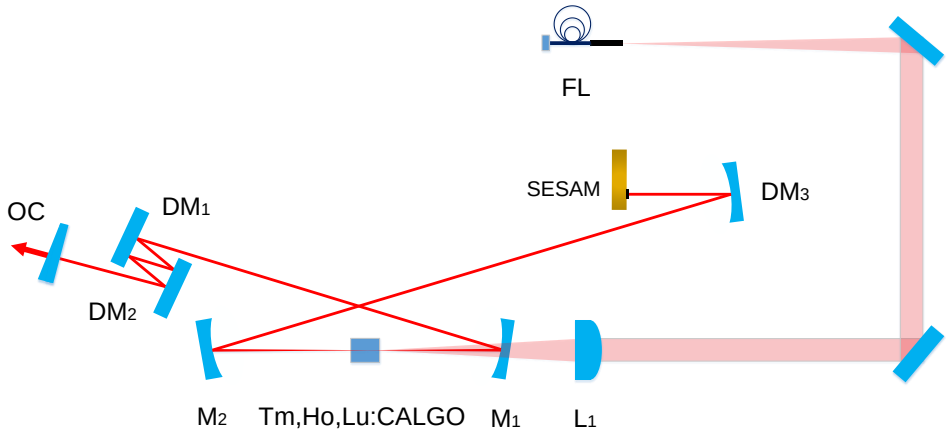

Figure 6. Experimental set up of the ML Tm,Ho,Lu:CALGO laser. Pump laser: Raman shifted Er Fiber Laser (FL); L_1: AR coated plano-convex lens (f = 75 mm); M_1-M_2: concave dichroic mirrors (RoC = −100 mm); DM_1 (flat), M_2 (flat) and M_3 (RoC = −100 mm): dispersive mirrors with GDD = −125 fs^2 per bounce; OC: wedged output coupler; SESAM: SEmiconductor Saturable Absorber Mirror.

Different GaSb based SESAMs with InGaAsSb quantum wells [25], OCs, and GDD values (by decreasing the number of bounces in Figure 6 or using DMs with higher negative GDD) were studied. The optimum SESAM for this laser in terms of stable ML operation and broad output spectra turned out to be one designed for the central wavelength of 2060 nm with two InGaAsSb quantum wells (thickness: 8.5 nm) and a 50 nm cap layer

without any AR coating [26]. The recovery measurements of the initial absorption by the pump-probe method at 2040 nm with 180-fs pulses indicated biexponential decay with intraband and interband relaxation times of 0.3 and 20 ps, respectively. The saturation fluence of such SESAMs is of the order of 10 μJ/cm^2, the modulation depth is 0.23% and the non-saturable losses are 0.12%.

Stable steady-state ML operation, though not self-starting, could be achieved only with the 0.2% OC. Higher *T*oc resulted in narrow output spectra at the optimum round trip GDD = −1250 fs^2. With the *T*oc = 0.2% OC the ML laser delivered a maximum average output power of 148 mW at the same absorbed pump power level of 3.84 W as in the CW reference measurement. Although the reduction of the output level compared to the CW regime is more than two times, at this low OC transmission, this confirms the relatively low (non-saturable) insertion losses of this SESAM. The increased losses and possibly the much broader spectral extend in the ML regime resulted in switching the output polarization of this laser to σ. This is consistent with our previous observations because the resulting central wavelength was below 2075 nm [23].

The optical spectrum of the ML Tm,Ho,Lu:CALGO laser shown in Figure 7a was centered at 2071.5 nm with a sech^2-fitted spectral FWHM of 21.5 nm. The corresponding autocorrelation trace measured by noncollinear Second-Harmonic Generation (SHG) is shown in Figure 7b. The fit assuming a sech^2-shaped pulse intensity gives a pulse duration (FWHM) of τ = 218 fs. The resulting time-bandwidth product (TBP) amounts to 0.327. It deviates only slightly from the 0.315 value for the ideal, unchirped sech^2-shaped pulses characteristic of a soliton laser. The soliton-like performance of this laser is confirmed by the almost ideal fitting of the spectral and temporal profiles in Figure 7. This pulse duration together with the average power give a peak power of roughly 7 kW.

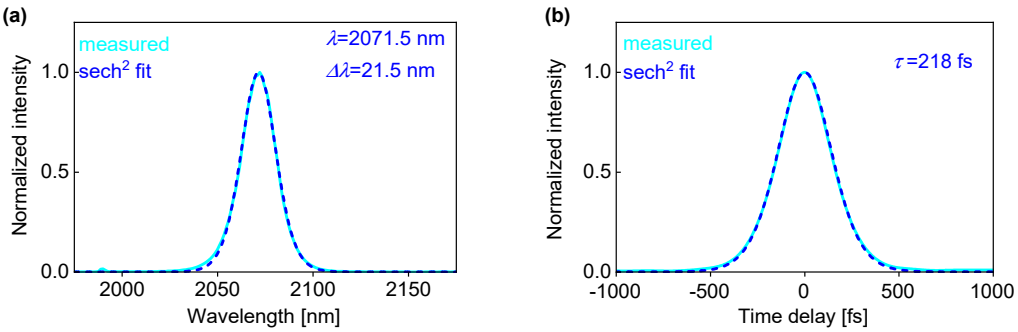

Figure 7. (**a**) Measured spectrum of the ML Tm,Ho,Lu::CALGO laser with T_{OC} = 0.2% and (**b**) second-harmonic generation (SHG) based background-free autocorrelation trace: experimental data and fitted curve assuming sech^2-shaped pulse intensity profile.

Figure 8a,b show the measured radio-frequency (RF) spectra of the fundamental beat note at ~96.2 MHz with a resolution bandwidth (RBW) of 300 Hz and a 1-GHz-wide span (RBW: 100 kHz) to verify the stability of the ML laser. The extinction ratio of more than 68 dBc and the absence of any spurious modulation are evidence for stable steady-state ML operation of the Tm,Ho,Lu:CALGO laser.

Attempts to further shorten the pulse duration with the optimum 0.2% OC were performed by modifying the cavity GDD. At a lower value of the negative round trip dispersion, e.g., −750 fs^2, the output spectrum broadened to 31 nm but no stable operation could be achieved.

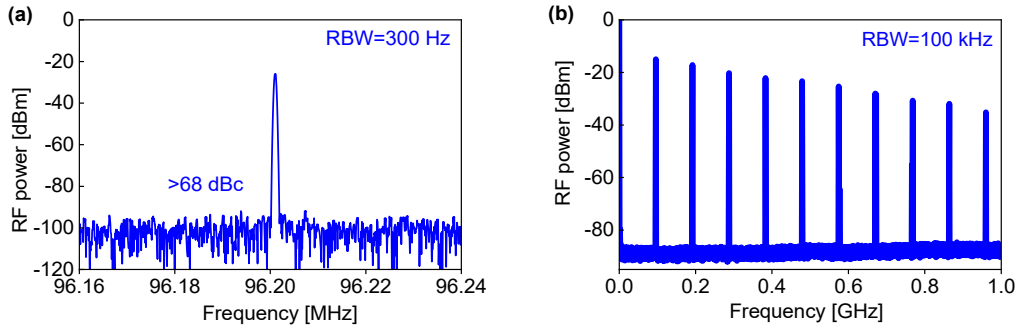

Figure 8. Radio-frequency (RF) spectra of the ML Tm,Ho,Lu:CALGO laser: (**a**) fundamental beat note measured with a resolution bandwidth (RBW) of 300 Hz and (**b**) a 1-GHz frequency span recorded with a RBM = 100 kHz. As established later, the decreasing intensity of the higher harmonics in (**b**) was, in fact, an artifact due to the low battery level of the detector used (ET-5000, EOT).

5. Conclusions

In-band pumping is a widespread method for pumping Ho lasers nowadays, thanks to the availability of well-developed Tm lasers operating at slightly shorter wavelengths and, in particular, commercial Tm-fiber lasers. While in-band pumping of Tm lasers has been, in general, also well-known, more sophisticated pump sources are needed, which are not readily available. In-band pumping has been employed also for Tm,Ho co-doped materials in the past; however, the main purpose was to increase the efficiency and the output power [24,27,28]. The main interest in the present study was to combine its potential with the utilization of the combined gain profile of the two ions, both for extended tunable operation and spectral support of shorter pulse durations in ML lasers. Using a home-made Raman shifted Er-fiber laser, we achieved a CW tuning range of 160 nm and a ML laser pulse duration of 218 fs. The latter is the first demonstration of a ML in-band pumped Tm,Ho laser, and thus represents an initial result. Based on our previous experience with utilization of the Kerr effect in the laser crystal for Kerr-lens mode locking assisted by a SESAM, we expect substantially shorter pulses in the range of 50 fs after optimization of the present set up. Concerning the material point of view, we also plan to study samples with increased Lu content as already demonstrated in the CW regime [22]. It should be outlined that the flipping of the polarization in such materials observed in CW operation and related to the close gain cross sections for the two principal polarizations offers another possibility for engineering of the actual gain profile in terms of full range, flatness, and smoothness by combining the two polarizations using a special crystal cut. We also plan to fully exploit the power scaling potential of the in-band pumping scheme by implementing more powerful pump sources in the future.

Author Contributions: Conceptualization, W.C. and R.T.M.; methodology, W.C., R.T.M., U.G. and L.W.; software, L.W. and W.C.; validation, W.C. and V.P.; formal analysis, H.Z. and W.C.; investigation, H.Z., W.X. and C.C.; resources, Z.P., P.L., X.M., R.T.M., U.G. and W.C.; data curation, H.Z., W.X., P.L., X.M. and C.C.; writing—original draft preparation, H.Z., W.X. and W.C.; writing—review and editing, V.P.; visualization, H.Z. and W.X.; supervision, W.C., R.T.M., L.W., U.G. and V.P.; project administration, V.P. and U.G.; funding acquisition, R.T.M. All authors have read and agreed to the published version of the manuscript.

Funding: We gratefully acknowledge support from the National Natural Science Foundation of China (Grants # 52072351, 61975208, 61905247, U21A20508); the Sino-German Scientist Cooperation and Exchanges Mobility Program (DFG Grant M-0040); MCIN/AEI/ 10.13039/501100011033 Grants PID2022-141499OB-I00 and PID2019-108543RB-I00; and the French Agence Nationale de la Recherche (ANR) SPLENDID2 (ANR-19-CE08-0028).

Data Availability Statement: The authors confirm that the data supporting the findings of this study are available within the article.

Acknowledgments: We gratefully acknowledge support from the Imperial College European Partners Fund and the Institute of Security Science and Technology Champions Fund. We thank Mircea Guina, Reflektron Ltd., Muotialankuja 5 C5, Tampere 33,800, Finland, for the provision of different GaSb-based SESAMs. We acknowledge also support from the Qilu Young Scholar Program of Shandong University and the Taishan Scholar Foundation of Shandong Province, as well as from the "RELANCE" Chair of Excellence project funded by the Normandy Region.

Conflicts of Interest: The authors declare no conflict of interest. The funders had no role in the design of the study; in the collection, analyses, or interpretation of data; in the writing of the manuscript; or in the decision to publish the results.

References

1. Petit, J.; Goldner, P.; Viana, B. Laser emission with low quantum defect in Yb:$CaGdAlO_4$. *Opt. Lett.* **2005**, *30*, 1345–1347. [CrossRef]
2. Hutchinson, J.A.; Verdun, H.R.; Chai, B.H.; Zandi, B.; Merkle, L.D. Spectroscopic evaluation of $CaYAlO_4$ doped with trivalent Er, Tm, Yb and Ho for eyesafe laser applications. *Opt. Mater.* **1994**, *3*, 287–306. [CrossRef]
3. Moncorgé, R.; Garnier, N.; Kerbrat, P.; Wyon, C.; Borel, C. Spectroscopic investigation and two-micron laser performance of Tm^{3+}:$CaYAlO_4$ single crystals. *Opt. Commun.* **1997**, *141*, 29–34. [CrossRef]
4. Shannon, R.D.; Oswald, R.A.; Parise, J.B.; Chai, B.H.T.; Byszewski, P.; Pajaczkowska, A.; Sobolewski, R. Dielectric constants and crystal structures of $CaYAlO_4$, $CaNdAlO_4$, and $SrLaAlO_4$, and deviations from the oxide additivity rule. *J. Sol. State Chem.* **1992**, *98*, 90–98. [CrossRef]
5. Vasylechko, L.; Kodama, N.; Matkovskii, A.; Zhydachevskii, Y. Crystal structure and optical spectroscopy of $CaGdAlO_4$:Er single crystal. *J. Alloys Compd.* **2000**, *300*, 475–478. [CrossRef]
6. Petit, P.O.; Petit, J.; Goldner, P.; Viana, B. Inhomogeneous broadening of optical transitions in Yb:$CaYAlO_4$. *Opt. Mater.* **2008**, *30*, 1093–1097. [CrossRef]
7. Loiko, P.; Druon, F.; Georges, P.; Viana, B.; Yumashev, K. Thermo-optic characterization of Yb:$CaGdAlO_4$ laser crystal. *Opt. Mater. Express* **2014**, *4*, 2241–2249. [CrossRef]
8. Loiko, P.; Serres, J.M.; Mateos, X.; Xu, X.; Xu, J.; Jambunathan, V.; Navratil, P.; Lucianetti, A.; Mocek, T.; Zhang, X.; et al. Microchip Yb:$CaLnAlO_4$ lasers with up to 91% slope efficiency. *Opt. Lett.* **2017**, *42*, 2431–2434. [CrossRef] [PubMed]
9. Loiko, P.; Becker, P.; Bohatý, L.; Liebald, C.; Peltz, M.; Vernay, S.; Rytz, D.; Serres, J.M.; Mateos, X.; Wang, Y.; et al. Sellmeier equations, group velocity dispersion and thermo-optic dispersion formulas for $CaLnAlO_4$ (Ln = Y, Gd) laser host crystals. *Opt. Lett.* **2017**, *42*, 2275–2278. [CrossRef] [PubMed]
10. Li, D.; Xu, X.; Cheng, Y.; Cheng, S.; Zhou, D.; Wu, F.; Xia, C.; Xu, J.; Zhang, J. Crystal growth and spectroscopic properties of Yb:$CaYAlO_4$ single crystal. *J. Cryst. Growth* **2010**, *312*, 2117–2121. [CrossRef]
11. Zaouter, Y.; Didierjean, J.; Balembois, F.; Lucas Leclin, G.; Druon, F.; Georges, P.; Petit, J.; Goldner, P.; Viana, B. 47-fs diode-pumped Yb^{3+}:$CaGdAlO_4$ laser. *Opt. Lett.* **2006**, *31*, 119–121. [CrossRef]
12. Sévillano, P.; Georges, P.; Druon, F.; Descamps, D.; Cormier, E. 32-fs Kerr-lens mode-locked Yb:$CaGdAlO_4$ oscillator optically pumped by a bright fiber laser. *Opt. Lett.* **2014**, *39*, 6001–6004. [CrossRef] [PubMed]
13. Druon, F.; Olivier, M.; Jaffrès, A.; Loiseau, P.; Aubry, N.; DidierJean, J.; Balembois, F.; Viana, B.; Georges, P. Magic mode switching in Yb:$CaGdAlO_4$ laser under high pump power. *Opt. Lett.* **2013**, *38*, 4138–4141. [CrossRef] [PubMed]
14. Beil, K.; Deppe, B.; Kränkel, C. Yb:$CaGdAlO_4$ thin-disk laser with 70% slope efficiency and 90 nm wavelength tuning range. *Opt. Lett.* **2013**, *38*, 1966–1968. [CrossRef]
15. Diebold, A.; Emaury, F.; Schriber, C.; Golling, M.; Saraceno, C.J.; Südmeyer, T.; Keller, U. SESAM mode-locked Yb:$CaGdAlO_4$ thin disk laser with 62 fs pulse generation. *Opt. Lett.* **2013**, *38*, 3842–3845. [CrossRef]
16. Petrov, V.; Wang, Y.; Chen, W.; Pan, Z.; Zhao, Y.; Wang, L.; Mero, M.; Choi, S.Y.; Rotermund, F.; Cho, W.B.; et al. Sub-100-fs bulk solid-state lasers near 2-micron. *Proc. SPIE* **2019**, *112094G*.
17. Di, J.; Xu, X.; Xia, C.; Sai, Q.; Zhou, D.; Lv, Z.; Xu, J. Growth and spectra properties of Tm, Ho doped and Tm, Ho co-doped $CaGdAlO_4$ crystals. *J. Lumin.* **2014**, *155*, 101–107. [CrossRef]
18. Liebald, C. Yb-dotierte Ultrakurzpuls-Lasermaterialien mit K_2NiF_4-Struktur—Züchtung und Verbesserung der Kristallqualität. Doctoral Dissertation, Johannes Gutenberg-Universität, Mainz, Germany, 2017. (In German).
19. Hu, Q.; Jia, Z.; Volpi, A.; Veronesi, S.; Tonelli, M.; Tao, X. Crystal growth and spectral broadening of a promising Yb:$CaLu_xGd_{1-x}AlO_4$ disordered crystal for ultrafast laser application. *CrystEngComm* **2017**, *19*, 1643–1647. [CrossRef]
20. Pan, Z.; Loiko, P.; Serres, J.M.; Kifle, E.; Yuan, H.; Dai, X.; Cai, H.; Wang, Y.; Zhao, Y.; Aguiló, M.; et al. "Mixed" Tm:Ca(Gd,Lu)AlO_4—A novel crystal for tunable and mode-locked 2 μm lasers. *Opt. Express* **2019**, *27*, 9987–9995. [CrossRef]
21. Pan, Z.; Loiko, P.; Slimi, S.; Yuan, H.; Wang, Y.; Zhao, Y.; Camy, P.; Dunina, E.; Kornienko, A.; Fomicheva, L.; et al. Tm,Ho:Ca(Gd,Lu)AlO_4 crystals: Crystal growth, structure refinement and Judd-Ofelt analysis. *J. Lumin.* **2022**, *246*, 118828. [CrossRef]
22. Pan, Z.; Loiko, P.; Serres, J.M.; Yuan, H.; Wang, Y.; Wang, L.; Zhao, Y.; Solé, R.M.; Aguiló, M.; Díaz, F.; et al. Tm,Ho:Ca(Gd,Lu)AlO_4 crystals: Polarized spectroscopy and laser operation. *J. Lumin.* **2023**, *257*, 119638. [CrossRef]

23. Wang, L.; Chen, W.; Zhao, Y.; Loiko, P.; Mateos, X.; Guina, M.; Pan, Z.; Mero, M.; Griebner, U.; Petrov, V. Sub-50 fs pulse generation from a SESAM mode-locked Tm,Ho-codoped calcium aluminate laser. *Opt. Lett.* **2021**, *46*, 2642–2645. [CrossRef] [PubMed]
24. Loiko, P.; Kifle, E.; Brasse, G.; Thouroude, R.; Starecki, F.; Benayad, A.; Braud, A.; Laroche, M.; Girard, S.; Gilles, H.; et al. In-band pumped Tm,Ho:$LiYF_4$ waveguide laser. *Opt. Express* **2022**, *30*, 11840–11847. [CrossRef]
25. Caird, J.A.; Payne, S.A.; Staver, P.R.; Ramponi, A.; Chase, L. Quantum electronic properties of the $Na_3Ga_2Li_3F_{12}$:Cr^{3+} laser. *IEEE J. Quantum Electron.* **1988**, *24*, 1077–1099. [CrossRef]
26. Paajaste, J.; Suomalainen, S.; Härkönen, A.; Griebner, U.; Steinmeyer, G.; Guina, M. Absorption recovery dynamics in 2 μm GaSb-based SESAMs. *J. Phys. D Appl. Phys.* **2014**, *47*, 065102. [CrossRef]
27. Kalachev, Y.L.; Mikhailov, V.A.; Podreshetnikov, V.V.; Shcherbakov, I.A. Study of a Tm,Ho:YLF laser pumped by a Raman shifted erbium-doped fiber laser at 1678 nm. *Quantum Electron.* **2010**, *40*, 296–300. [CrossRef]
28. Kifle, E.; Loiko, P.; Romero, C.; de Aldana, J.R.V.; Zakharov, V.; Gurova, Y.; Veniaminov, A.; Petrov, V.; Griebner, U.; Thouroude, R.; et al. Tm^{3+} and Ho^{3+} colasing in in-band pumped waveguides fabricated by femtosecond laser writing. *Opt. Lett.* **2021**, *46*, 122–125. [CrossRef]